Check for updates

Water Reuse

IWA PUBLISHING

© 2021 The Authors

Water Reuse Vol 11 No 4, 560 doi: 10.2166/wrd.2021.053

Kinetics of diatrizoate degradation by ozone and the formation of disinfection by-products in the sequential chlorination

Chen-Yan Hu[a,b], Si-Cheng Ren[a], Yi-Li Lin[c,*], Ji-Chen Zhang[a], Ye-Ye Zhu[a], Cun Xiong[a] and Qiang-Bin Wang[a]

[a] College of Environmental and Chemical Engineering, Shanghai Engineering Research Center of Energy-Saving in Heat Exchange Systems, Shanghai University of Electric Power, Shanghai 200090, China
[b] Shanghai Institute of Pollution Control and Ecological Security, Shanghai 200092, China
[c] Department of Safety, Health and Environmental Engineering, National Kaohsiung University of Science and Technology, Kaohsiung 824, Taiwan, ROC
*Corresponding author. E-mail: yililin@nkust.edu.tw

Y-LL, 0000-0003-3426-3565; J-CZ, 0000-0002-1930-8174

ABSTRACT

In this study, we studied the degradation kinetics of a common iodine contrast agent, diatrizoate, by ozone and the formation of disinfection by-products (DBPs) in the sequential chlorination. Effects of ozone concentration, solution pH, and bromide concentration on diatrizoate degradation were evaluated. The results indicate that diatrizoate can be effectively degraded (over 80% within 1 h) by ozone, and the degradation kinetics can be well described using the pseudo-first-order kinetic model. The pseudo-first-order rate constant (k_{obs}) of diatrizoate degradation significantly increased with increasing ozone concentration and decreasing bromide concentration. The k_{obs} kept increasing with the increase of pH value and reached a maximum of 6.5 ($\pm$0.05) $\times$ 10^{-2} min^{-1} at pH 9. As the ozone concentration gradually increased from 0.342 to 1.316 mg/L, the corresponding k_{obs} of diatrizoate degradation increased from 1.76 ($\pm$0.20) $\times$ 10^{-3} to 4.22 ($\pm$0.3) $\times$ 10^{-2} min^{-1}. The bromide concentration exhibited a strong inhibitory effect on diatrizoate degradation because of the competition for ozone with diatrizoate. Trichloromethane was the only detected DBP in the subsequent chlorination in the absence of bromide. However, in the presence of bromide, six other DBPs were detected, and bromochloroiodomethane and tribromomethane became the major products with concentrations 1–2 orders higher than those of the other DBPs. In order to provide safe drinking water to the public, water should be maintained at circumneutral pH values and low bromine concentrations (<5 μM) before reaching the chlorine disinfection process to effectively control the formation of DBPs.

Key words: bromide, chlorine, disinfection by-product (DBP), iodinated X-ray contrast media (ICM), kinetics, ozone

HIGHLIGHTS

- Diatrizoate ozonation followed pseudo-first-order kinetics.
- The diatrizoate degradation rate can be significantly increased at pH > 7.
- •OH played a major role in diatrizoate degradation during ozonation.
- Bromide can strongly inhibit diatrizoate degradation because of the competition for ozone with diatrizoate.
- The formation of DBPs can be controlled at circumneutral pH and low bromine concentrations (<5 μM).

This is an Open Access article distributed under the terms of the Creative Commons Attribution Licence (CC BY 4.0), which permits copying, adaptation and redistribution, provided the original work is properly cited (http://creativecommons.org/licenses/by/4.0/).

Downloaded from http://iwa.silverchair.com/jwrd/article-pdf/11/4/560/973551/jwrd0110560.pdf
by guest

GRAPHICAL ABSTRACT

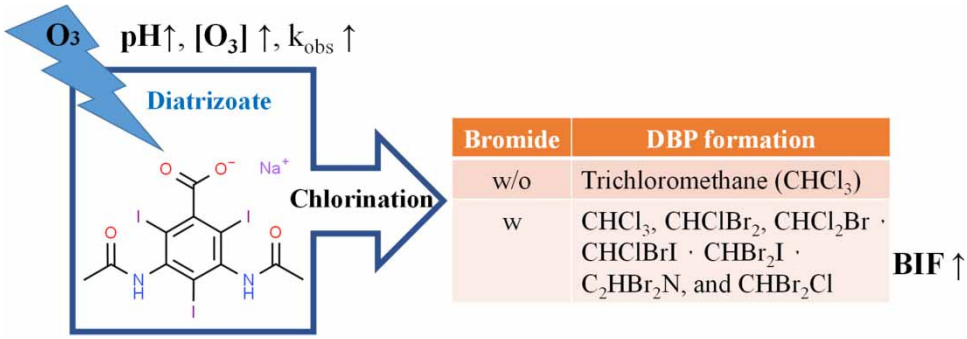

1. INTRODUCTION

Iodinated X-ray contrast media (ICM) are a class of pharmaceutical products widely used to increase the contrast of tissue, structures, and details of organs and blood vessels during medical imaging at hospitals and medical centers (Hu *et al.* 2019a). The annual global consumption of ICM is approximately 3.5×10^6 kg (Perez & Barcelo 2007; Wang *et al.* 2016), and the annual estimated production of ICM is more than 5×10^6 kg (Gharekhanloo & Torabian 2012; Hu *et al.* 2019a). Typically, 95% of non-metabolized ICM can be eliminated through urine and feces within 24 h after adoption (Sandra Perez *et al.* 2006). The molecular structures of ICM consist of 2,4,6-triiodinated benzoic derivatives, and their molecular weights vary between 600 and 900 Da (Jeong *et al.* 2017). The structures of ICM are very stable and cannot be effectively removed by traditional water treatment processes (Hu *et al.* 2020a). Therefore, trace amounts of ICM are commonly detected in surface waters (Duirk *et al.* 2011; Kormos *et al.* 2011). In a previous study, many kinds of ICM were detected in the rivers (Duirk *et al.* 2011) of drinking water sources in the US at the levels of 10–2,700 ng/L, including iopamidol, iomeprol, iopromide, iohexol, and diatrizoate.

ICM can be divided into ionic and nonionic groups (Hu *et al.* 2019b), which are all commonly used ICM nowadays (Hu *et al.* 2020b). Diatrizoate is a nonionic ICM that is especially resistant to conventional wastewater and drinking water treatment processes (Sugihara *et al.* 2013). Therefore, many researchers have focused on the degradation of diatrizoate using advanced oxidation techniques (Hennebel *et al.* 2010; Velo-Gala *et al.* 2014; Azerrad *et al.* 2016; Polo *et al.* 2016; Meng *et al.* 2017). For example, Hennebel *et al.* (2010) removed diatrizoate using a catalytically active membrane, and the removal efficiency reached 77% after 48 h. Velo-Gala *et al.* (2014) compared the degradation of diatrizoate in a solution with various advanced oxidation processes (AOPs) using iron salts and ultraviolet light (UV) radiation. Experimental results showed that UV/$K_2S_2O_8$ is more effective than UV/H_2O_2 with a higher reaction rate constant for diatrizoate degradation. Polo *et al.* used solar radiation to degrade diatrizoate (Polo *et al.* 2016) and reported that the formation of free radical promoting substances (including complexes of peroxygen and iron hydroperoxide) can absorb radiation in the solar radiation area, resulting in 100% sunlight degradation of diatrizoate. A German municipal sewage treatment plant (STP) using ozonation only achieved 14% removal of diatrizoate (Ternes *et al.* 2003).

Halogenated disinfection by-products (DBPs) are produced by natural organic matter (NOM) reacting with chlorine during drinking water disinfection (Jiang *et al.* 2020). The presence of ICM in the source water may also react with chlorine to produce highly toxic iodinated DBPs (I-DBPs), which have aroused high concerns for public health (Jeong *et al.* 2017). DBPs have chronic cytotoxicity and genomic induction. Research results indicated that 13 kinds of haloacetamides can damage the DNA of Chinese hamster ovary cells (Michael *et al.* 2008). Moreover, Jiang *et al.* (2017) reported that the presence of bromide ions in the raw water may participate in the reactions between NOM and chlorine to generate brominated-DBPs (Br-DBPs), which are more carcinogenic and mutagenic than their chlorinated analogues. Epidemiological studies have consistently observed a correlation between chlorine consumption in drinking water and increasing risk of bladder cancer (Li & Mitch 2018). DBPs and their toxic effects will put pressure on the living creatures in the environment and organisms (Shang *et al.* 2019; Ranjan *et al.* 2021). ICM is a potential source of toxic I-DBPs during water disinfection, such as iopamidol (Mao *et al.* 2020). It has been reported that I-DBPs are generated during chlorine disinfection of iodide-containing water in sewage treatment systems (Allard *et al.* 2013; Xia *et al.* 2017; Liu *et al.* 2018; Zhang *et al.* 2019). Allard *et al.* (2013) reported that in

Downloaded from http://iwa.silverchair.com/jwrd/article-pdf/11/4/560/973551/jwrd0110560.pdf
by guest

iodide-containing waters, I-DBPs can be produced during chlorination or especially chloramination; a pre-ozonation step to oxidize iodide to iodate is an efficient process to mitigate I-DBP formation. I-DBPs have recently become an emerging group of DBPs with public health concerns (Yolanta *et al.* 2014). To the authors' best knowledge, no literature regarding the degradation kinetics of diatrizoate ozonation and DBP formation after post-chlorination have been reported, which are worth research attention in order to provide safe drinking water to the public.

Therefore, the purposes of this study were (1) to investigate the kinetics of diatrizoate degradation during ozone oxidation, (2) to evaluate the effects of bromide concentration and solution pH on diatrizoate degradation, and (3) to investigate the formation of regulated and emerging DBPs of ozonated diatrizoate in the subsequent chlorination to simulate water distribution in the pipelines.

2. MATERIALS AND METHODS

2.1. Chemicals and reagents

Diatrizoate (>99.0%) was obtained from Sigma-Aldrich (St. Louis, MO, USA). Sodium bromide (NaBr), potassium iodide (KI), sodium bicarbonate ($NaHCO_3$), nitrobenzene ($C_6H_5NO_2$), tert-butanol (C_4H_9OH, TBA), sodium carbonate (Na_2CO_3), potassium dihydrogen phosphate (KH_2PO_4), sodium thiosulfate ($Na_2S_2O_3$), methanol (CH_4O), sodium hydroxyl (NaOH), and hydrochloric acid (HCl) were acquired from Sinopharm Chemical Reagent Co., Ltd (Shanghai, China). US EPA 551A and 551B halogenated DBP standard solutions, including trihalomethanes (THMs) and haloacetonitriles, were purchased from Sigma-Aldrich (USA). Other standard solutions of iodinated trihalomethanes (I-THMs), including CHI_3, $CHBr_2I$, CHBrClI, $CHBrI_2$, $CHCl_2I$, and $CHClI_2$ were purchased from CanSyn Chemical Corporation (Toronto, ON, Canada). Methyl tert-butyl ether (MtBE) was purchased from J.T. Baker (USA). Ultrapure water produced by a Milli-Q water purification system (Millipore, USA) was used in the experiments to prepare the solutions. All chemicals were at least at analytical purity, and all solvents are at high-performance liquid chromatograph (HPLC) grade and used without further purification.

2.2. Ozone reaction system

The schematic diagram of the ozone reaction system is displayed in Figure 1. Ozone gas was produced by a COM-AD-01 ozone generator (Anseros, Germany). The desired ozone concentration was controlled by adjusting the flow rate of a stream of pure ozone gas into the reactor. Before each experiment, the concentration of dissolved ozone in the reactor was monitored by measuring the amount of I_2 formed in the reaction between O_3 and potassium iodide solution according to the sodium thiosulfate titration method based on the following equations (Giuseppe *et al.* 2007).

$$O_3 + 2KI + H_2O \rightarrow O_2 + I_2 + 2KOH \quad (1)$$

$$I_2 + 2Na_2S_2O_3 \rightarrow 2NaI + Na_2S_4O_6 \quad (2)$$

An internal micro pump (MP-10R, Keyuan Pumps Co., Ltd, Shanghai, China) and an external peristaltic pump (DP-130, Shanghai Magnetic Pump Co., Ltd, Shanghai, China) were adopted to circulate the water inside the double-layer glass reactor and the water flowed in the outer layer, respectively, to maintain the system temperature at 25 ± 1 °C.

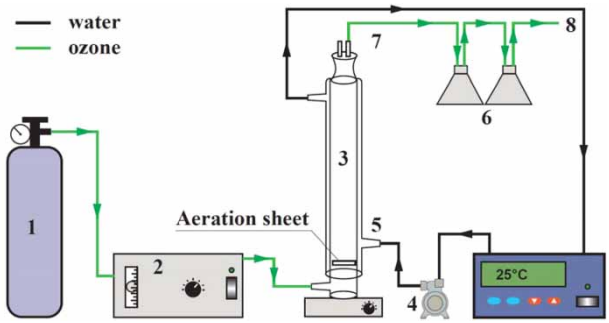

Figure 1 | Schematic diagram of the experimental setup of the ozonation system. 1. High purity oxygen cylinder, 2. Ozone generator, 3. Double-layer glass reactor, 4. Circulating pump, 5. Water bath, 6. Tail gas absorption bottle, 7. Drain outlet, 8. Sampling port.

Downloaded from http://iwa.silverchair.com/jwrd/article-pdf/11/4/560/973551/jwrd0110560.pdf
by guest

2.3. Experimental procedures

The ozonation experiments were carried out in a ventilated hood. Diatrizoate stock solution (1 mM) was prepared to make each reacting solution of 20 μM and 200 mL using ultrapure water. The pH value of the reaction solution was adjusted to a desired value (pH 5–9) by adding a small amount (<5 mL) of H_2SO_4 (0.18M) or NaOH (1M) in the presence of 10 mM phosphate buffer. In order to ensure the purity of the produced ozone, the ozone gas produced by the generator was pre-ventilated for 30 min into a saturated potassium iodide solution to adsorb ozone before releasing into the atmosphere. After pre-aeration, the pure ozone gas was passed into the double-layer reactor to start the reaction. For the kinetic experiments, the ozone concentrations were set at 0.342–1.316 mg/L, while for the degradation experiments, the O_3 concentration was fixed at 0.713 mg/L. At a certain time interval, 1 mL of the reaction solution was taken from the sampling port and transferred into an HPLC vial containing $Na_2S_2O_3$ (concentration more than 1.2 times the ozone concentration) to quench the reaction, and the sample was stored at 4 °C in the dark for analyzing the residual diatrizoate concentration using an HPLC as soon as possible. Parallel experiments were performed simultaneously. On the other hand, TBA with concentration more than 1.2 times the ozone concentration was dosed in the solution to verify the contribution of hydroxyl radicals (•OH) on diatrizoate degradation during ozonation.

To study the effect of bromide concentration on diatrizoate degradation, the experiments were performed by dosing bromide concentrations of 0–150 μM at pH 7 and ozone concentration of 0.713 mg/L. For the evaluation of DBP formation after diatrizoate ozonation in the sequential chlorination to simulate drinking water distribution in the pipelines, the diatrizoate solution was prepared in a 45 mL vial dosing 100 μM free chlorine, sealed and preserved in a thermostatic incubator at 25 °C for 3 d. Then, all samples were quenched with $Na_2S_2O_3$. Each DBP formation experiment was performed in duplicate with averaged values being reported in this study.

2.4. Analytical methods

An Agilent 1200 infinity series HPLC system (Agilent, USA) was used to analyze the concentration of diatrizoate with an XTerra MS C18 column (5 μm, 250 mm × 4.6 mm, Waters, USA), a UV detector, and an autosampler with an injection volume of 5 μL. The mobile phase was composed of 10%/90% (v/v) methanol and 1% phosphoric acid solution (v/v) at a flow rate of 1 mL min^{-1}, and the volume ratio is 10%/90%. The detection wavelength of diatrizoate was 237 nm.

A GC (GC-2010 Plus, Shimadzu, Japan) equipped with an RTX-5 fused-silica capillary column (30 m × 0.25 mm id, 0.25 μm film thickness) and an electron capture detector was used to analyze the concentrations of the formed DBPs. The analysis was conducted according to the US EPA method 551.1 (Richardson *et al.* 2007).

3. RESULTS AND DISCUSSION

3.1. Kinetics of diatrizoate degradation during ozone oxidation

Figure 2 displays the pseudo-first-order kinetics plot of diatrizoate degradation during ozonation with different initial ozone concentrations. Diatrizoate can be degraded by more than 91% after 60 min ozonation. The fitted line in Figure 2 exhibited a high linearity ($R^2 > 0.99$), indicating that diatrizoate degradation follows pseudo-first-order kinetics during ozonation. The degradation rate of diatrizoate can be expressed as follows:

$$\frac{-d[\text{Diatrizoate}]}{dt} = k_{\text{obs}}[\text{Diatrizoate}] \tag{3}$$

where [Diatrizoate] represents the diatrizoate concentration at time t, and k_{obs} (min^{-1}) represents the observed pseudo-first-order rate constant of diatrizoate degradation during ozonation.

The slope in Figure 2 is k_{obs}. As the initial ozone concentration increased from 0.342 to 1.316 mg/L, k_{obs} increased linearly from 1.76 ($\pm$0.20) × 10^{-3} to 4.22 ($\pm$0.3) × 10^{-2} min^{-1} ($R^2 > 0.923$), which can be explained by the increasing concentrations of dissolved ozone and the resulted hydroxyl radicals in the solution (Huang *et al.* 2020a). Therefore, the ozonation degradation of diatrizoate can be further expressed as follows:

$$\frac{-d[\text{Diatrizoate}]}{dt} = k_{\text{obs}}[\text{Diatrizoate}] = k_{\text{app}}[O_3][\text{Diatrizoate}] \tag{4}$$

Downloaded from http://iwa.silverchair.com/jwrd/article-pdf/11/4/560/973551/jwrd0110560.pdf
by guest

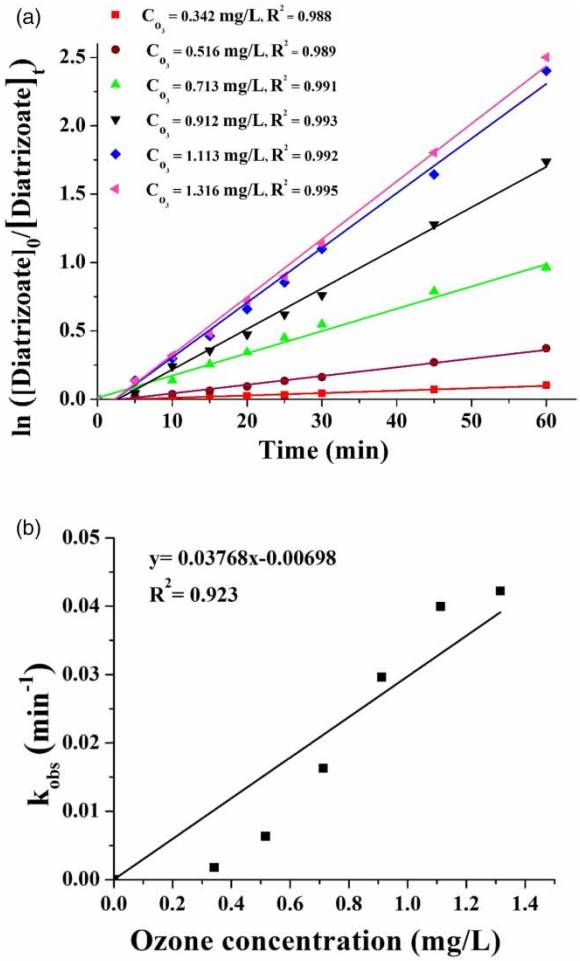

Figure 2 | (a) Pseudo-first-order kinetics plot of diatrizoate degradation at different ozone concentrations, [diatrizoate]0 = 20 μM, [phosphate buffer]0 = 10 mM, and temperature = 25 °C. (b) Correlation between k_{obs} and ozone concentration.

where k_{app} represents the apparent second-order reaction rate constant of the entire reaction. In sum, the ozonation degradation of diatrizoate fitted the second-order kinetics well, one order in ozone concentration and one order in diatrizoate concentration. The relationship between k_{obs} and k_{app} can be expressed (Equation (5)) and calculated as 0.03768 L (min mg)$^{-1}$, which is higher than that of iohexol degradation during ozonation (Hu *et al.* 2020a).

$$k_{app} = \frac{k_{obs}}{[O_3]_T} = 0.03768 \quad (5)$$

3.2. Effect of tert-butanol (TBA) on diatrizoate degradation during ozonation

In order to verify the contribution of hydroxyl radicals (•OH) on diatrizoate degradation during ozonation, the commonly used quencher, TBA, was dosed during the reaction. As displayed in Figure 3(a) and 3(b), the degradation rate of diatrizoate decreased sharply in the absence of TBA, while the degradation rate of diatrizoate only slightly decreased in the presence of TBA. Therefore, it can be concluded that •OH played the major role in diatrizoate degradation during ozonation along with partial contribution of ozone and other radicals.

3.3. Effect of solution pH on the degradation of diatrizoate during ozonation

The effect of solution pH on diatrizoate degradation during ozonation was investigated at pH 5.5–9, and the results are presented in Figure 4. The degradation rate of diatrizoate gradually increased from 4.17 ($\pm$0.04) $\times$ 10^{-3} min^{-1} to the maximum

Downloaded from http://iwa.silverchair.com/jwrd/article-pdf/11/4/560/973551/jwrd0110560.pdf
by guest

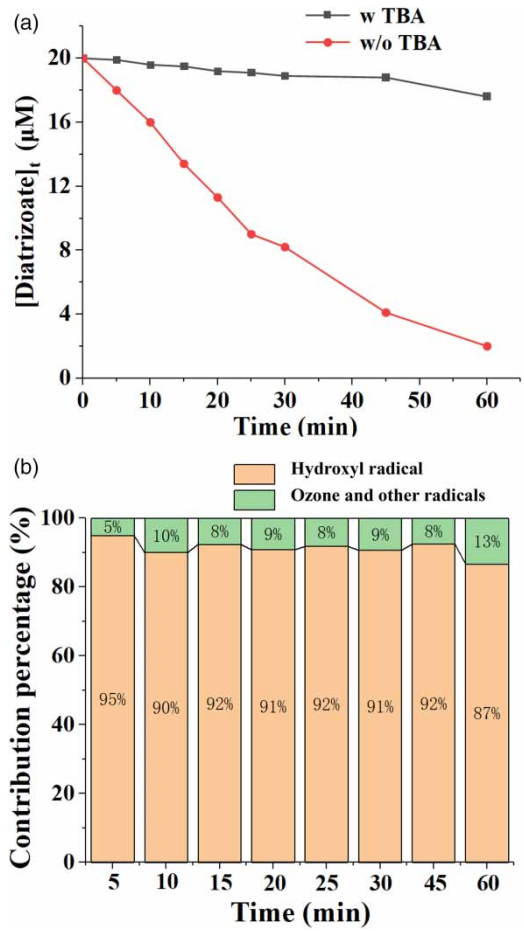

Figure 3 | (a) Effect of tert-butanol on the degradation of diatrizoate during ozonation, [Ozone] = 0.713 mg/L, [diatrizoate]0 = 20 μM, [phosphate buffer]0 = 10 mM, [TBA] = 0.856 mg/L, and temperature = 25 °C. (b) Contribution percentage of different radicals to diatrizoate degradation.

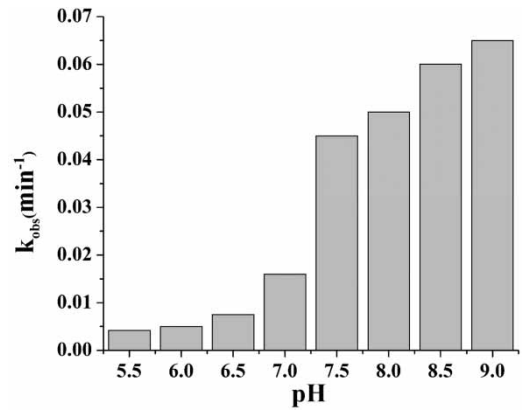

Figure 4 | Effect of solution pH on the rate constant of diatrizoate degradation during ozonation, [Ozone] = 0.713 mg/L, [diatrizoate]0 = 20 μM, [phosphate buffer] 0 = 10 mM, and temperature = 25 °C.

of 6.5 ($\pm$0.05) $\times$ 10^{-2} min^{-1} as pH increased from 5.5 to 9.0. The dosed diatrizoate can be completely decomposed at pH 7.5–9.0 within an hour. The rate constants of diatrizoate degradation during ozonation in alkaline conditions were significantly higher than those in acidic conditions. This phenomenon can be explained by the major contribution of hydroxyl radicals

Downloaded from http://iwa.silverchair.com/jwrd/article-pdf/11/4/560/973551/jwrd0110560.pdf
by guest

(•OH) to diatrizoate degradation, which will be further discussed in Section 3.5. At pH > 7, increasing OH^- concentration in the solution can promote the formation of hydroxyl radicals according to Equations (6) and (7). A series of reactions can happen with the generation of other active radicals at different pH values, such as •OH, O_2^-•, O_3^-•, HO_3•, O^-•, and HO_2•(Equations (8)–(13)). Therefore, the pH of the solution played an important role in diatrizoate degradation during ozonation (Gunten 2003; Virmani *et al.* 2020).

$$O_3 + OH^- \rightarrow HO_2^- + O_2, \quad k = 4.2 \times 10^2\ M^{-1}\ min^{-1} \tag{6}$$

$$O_3 + HO_2^- \rightarrow \bullet OH + O_2^-\bullet + O_2, \quad k = 1.68 \times 10^8\ M^{-1}\ min^{-1} \tag{7}$$

$$O_3 + O_2^-\bullet \rightarrow O_3^-\bullet + O_2, \quad k = 9.6 \times 10^{10}\ M^{-1}\ min^{-1} \tag{8}$$

$$\text{at pH} \leq 7.5: \quad O_3^-\bullet + H^+ \rightleftharpoons HO_3\bullet \tag{9}$$

$$HO_3\bullet \rightarrow \bullet OH + O_2 \tag{10}$$

$$\text{at pH} \geq 7.5: \quad O_3^-\bullet \rightleftharpoons O^-\bullet + O_2 \tag{11}$$

$$O^-\bullet + H_2O \rightarrow \bullet OH + OH^- \tag{12}$$

$$\bullet OH + O_3 \rightarrow HO_2\bullet + O_2 \tag{13}$$

3.4. Effects of bromide concentration on diatrizoate degradation during ozonation

Figure 5(a) and 5(b) displays the effect of bromide concentration on the degradation of diatrizoate. It is obvious that the rate of diatrizoate degradation significantly decreased as the bromide concentration increased in the solution. The reason is that Br^- can compete with diatrizoate for ozone consumption and cause a series of chain reactions (Equations (14)–(20); Song *et al.* 1996). Solutions containing Br^- are prone to form BrO_3^- during ozonation (Equation (18)), which has weak oxidizing power for organic compounds (Gunten 2003; Nie *et al.* 2013). Although in Equation (16), a strong oxidant HOBr and several bromine radicals can be formed, a part of them can further react with •OH to form BrO^- and BrO_2^- (Equations (17)–(20)), which are also weak oxidants (Huang *et al.* 2020b). Therefore, the presence of bromide exhibited an inhibitory effect on diatrizoate degradation during ozonation.

$$2Br^- + 2O_3 \rightarrow 2Br\bullet + 3O_2 \tag{14}$$

$$Br\bullet + Br^- \rightarrow Br_2^-\bullet, \quad k = 6 \times 10^{12}\ M^{-1}\ min^{-1} \tag{15}$$

$$Br_2^-\bullet + 3O_3 + H_2O \rightarrow 2HOBr + 4O_2 \tag{16}$$

$$HOBr + O_3 \rightarrow HBrO_2 + O_2 \tag{17}$$

$$HOBr + 2O_3 \rightarrow HBrO_3 + 2O_2 \tag{18}$$

$$Br_2^-\bullet + Br_2^-\bullet \rightarrow Br^- + Br_3^-\bullet, \quad k = 1.2 \times 10^{11}\ M^{-1}\ min^{-1} \tag{19}$$

$$Br_3^-\bullet + H_2O \rightarrow HOBr + H^+ + 2Br^- \tag{20}$$

3.5. Effect of solution pH on DBP formation of ozonated diatrizoate in the sequential chlorination

In previous literature, pH can have significant effects on DBP formation during disinfection (especially using chlorine). Therefore, DBP formation potential of diatrizoate after ozonation was also evaluated after 3 d chlorination to simulate water distribution in pipelines. As shown in Figure 6 in the absence of bromide, only trichloromethane ($CHCl_3$) was detected in the sequential chlorine process. Due to the strong oxidizing ability of ozone and •OH, diatrizoate can be decomposed into small molecular structures. ICMs can be degraded to a different extent during AOPs to form inorganic iodine and organic iodide at pH >7 (Ina *et al.* 2009), and ozone can oxidize iodide ions to HOI (Equations (21) and (22)) that can further react with O_3 to generate IO_2^- and IO_3^- (Equations (23) and (24)). Therefore, iodate will be the major product during

Downloaded from http://iwa.silverchair.com/jwrd/article-pdf/11/4/560/973551/jwrd0110560.pdf
by guest

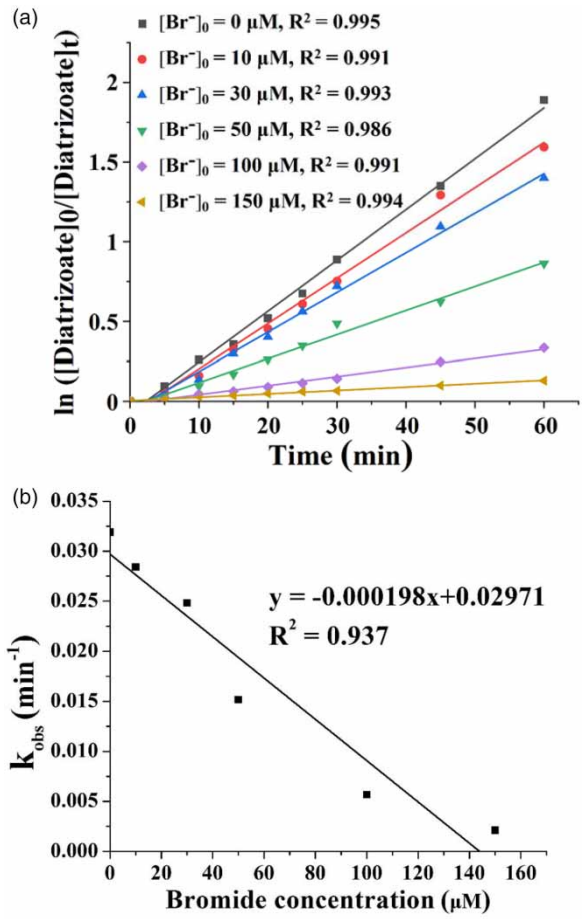

Figure 5 | (a) Pseudo-first-order kinetics plot of diatrizoate degradation at different bromine concentrations during ozonation at pH 7, [ozone] = 0.713 mg/L, [diatrizoate]0 = 20 μM, [phosphate buffer]0 = 10 mM, and temperature = 25 °C. (b) Correlation between k_{obs} and bromide concentration.

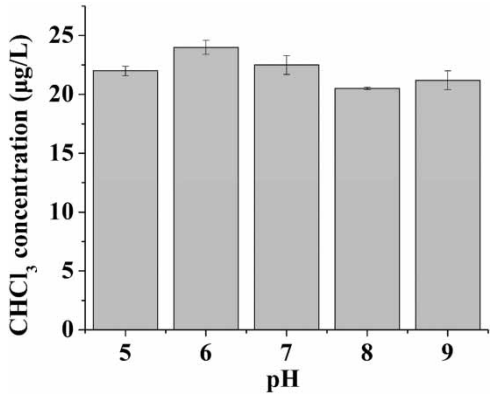

Figure 6 | DBP formation of ozone oxidized diatrizoate after 3 d chlorination at pH 5–9, [diatrizoate]0 = 20 μM, [ozone] = 0.713 mg/L, [HOCl]0 = 100 μM, [phosphate buffer]0 = 10 mM, and temperature = 25 °C.

Downloaded from http://iwa.silverchair.com/jwrd/article-pdf/11/4/560/973551/jwrd0110560.pdf
by guest

the ozone disinfection process without forming a considerable amount of I-DBPs (Von 2003).

$$I^- + O_3 \rightarrow OI^- + O_2, \quad k = 9.6 \times 10^7\ M^{-1}\ min^{-1} \tag{21}$$

$$H^+ + OI^- \rightarrow HOI, \quad k = 2.16 \times 10^6\ M^{-1}\ min^{-1} \tag{22}$$

$$OI^- + O_3 \rightarrow IO_2^- + O_2 \tag{23}$$

$$IO_2^- + O_3 \rightarrow IO_3^- + O_2 \tag{24}$$

3.6. Effects of bromide concentration on the formation of DBPs after post-chlorination

Figure 7 displays the effect of bromide concentration on the formation of DBPs after chlorination of ozone oxidized diatrizoate. It can be seen that six more kinds of DBPs besides $CHCl_3$ were detected, including $CHClBr_2$, $CHCl_2Br$, CHClBrI, $CHBr_2I$, C_2HBr_2N, and $CHBr_2Cl$, and the dominant one was CHClBrI. As the bromide concentration increased from 5 to 200 μM, C_2HCl_3, C_2HBrN, and $CHClBr_2$ formation remained relatively low and stable. However, the concentrations of $CHBr_3$ increased with increasing bromine concentration, while the concentrations of two detected I-DBPs, $CHBr_2I$, and CHClBrI exhibited an increasing and then decreasing trend. As the bromide concentration reached 100 μM, $CHBr_2I$ was detected. Accordingly, the presence of Br^- has a considerable impact on the production of DBPs. In order to analyze the contribution of bromine to the formation of THMs, the bromine incorporation factor (BIF) was calculated according to the following equation:

$$BIF = Br^{atom}_{number\ x}[Br - THMs]/[\text{total THM species}] \tag{25}$$

The range of BIF is 0–3 (Rathbun 1996). The larger the BIF value, the greater the contribution of bromine to the formation of THMs, indicating the greater proportion of Br-THMs in the total concentration of THMs. As the concentration of bromide increased from 10 to 200 μM, the BIF increased from 1.15 to 2.01, implying that Br-DBPs were preferentially produced, and chlorinated-DBPs were inhibited in the presence of bromide in the subsequent chlorination after diatrizoate ozonation (Ates *et al.* 2007). The presence of Br^- in the solution can react with HOCl to form HOBr (Cowman & Singer 1996; Brix *et al.* 2017), which is a strong oxidizing agent with oxidation power stronger than that of HOCl (Symons *et al.* 1993; Maryam *et al.* 2020) and can react with diatrizoate or its degradation intermediates at higher reaction rates (Chang *et al.* 2001), causing more formation of Br-DBPs (and even I-DBPs) with higher toxicity. Therefore, although ozone is efficient to decompose diatrizoate, it is essential to control the potential risks of forming toxic Br-DBPs and I-DBPs in the presence of bromide in the sequential chlorination.

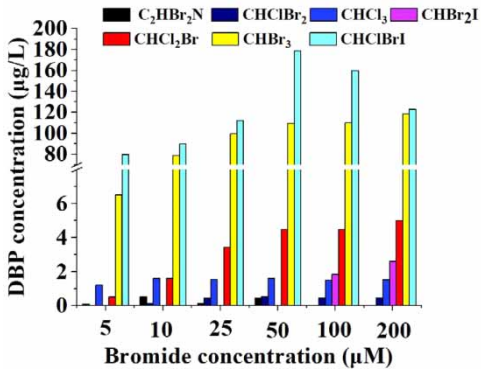

Figure 7 | DBP formation of oxidized diatrizoate after 3 d chlorination ozonation at different bromide concentrations, [diatrizoate]0 = 20 μM, [ozone] = 0.713 mg/L, [HOCl]0 = 100 μM, [phosphate buffer]0 = 10 mM, pH = 7, and temperature = 25 °C.

Downloaded from http://iwa.silverchair.com/jwrd/article-pdf/11/4/560/973551/jwrd0110560.pdf
by guest

4. CONCLUSION

This study shows the successful application of ozone to completely decompose diatrizoate in alkaline conditions. Diatrizoate degradation during ozonation followed pseudo-first-order kinetics well. •OH played a major role in the diatrizoate degradation process, which was confirmed by the quenching experiments using TBA. At 25 °C, the degradation rate of diatrizoate by ozonation increased with increasing solution pH and ozone concentration. In the sequential chlorination simulating for water distribution in the pipelines, only one DBP, $CHCl_3$, was detected, and its formation was not pH-dependent. On the other hand, as Br^- concentration increased, the diatrizoate degradation efficiency decreased significantly due to the competition of ozone with diatrizoate, and six more kinds of DBPs were detected in the water after post-chlorination. Moreover, as Br^- concentration increased to 100 μM, Br-DBPs were preferentially produced, and $CHBr_2I$ was detected. Therefore, although ozone is efficient to decompose diatrizoate, it is essential to control the potential risks of forming toxic Br-DBPs and I-DBPs in the presence of bromide in the sequential chlorination.

ACKNOWLEDGEMENTS

This study was supported by the Natural Science Foundation of China (Grant No. 52170006), Shanghai Committee of Science and Technology, China (Grant No. 17DZ2282800), and the Ministry of Science and Technology, Taiwan (MOST-110-2221-E-992-025).

DATA AVAILABILITY STATEMENT

All relevant data are included in the paper or its Supplementary Information.

REFERENCES

Allard, S., Nottle, C. E., Chan, A., Joll, C. & Gunten, U. V. 2013 Ozonation of iodide-containing waters: selective oxidation of iodide to iodate with simultaneous minimization of bromate and I-THMs. *Water Res.* **47**, 1953–1960.

Ates, N., Yetis, U. & Kitis, M. 2007 Effects of bromide ion and natural organic matter fractions on the formation and speciation of chlorination by-products. *J. Environ. Eng.* **133**, 947–954.

Azerrad, S. P., Lutke Eversloh, C., Gilboa, M., Schulz, M., Ternes, T. & Dosoretz, C. G. 2016 Identification of transformation products during advanced oxidation of diatrizoate: effect of water matrix and oxidation process. *Water Res.* **103**, 424–434.

Brix, K., Hein, C., Sander, J. M. & Kautenburger, R. 2017 Simultaneous quantification of iodine and high valiant metals via ICP-MS under acidic conditions in complex matrices. *Talanta* **167**, 532–536.

Chang, E. E., Lin, Y. P. & Chiang, P. C. 2001 Effects of bromide on the formation of THMs and HAAs. *Chemosphere* **43**, 1029–1034.

Cowman, G. A. & Singer, P. C. 1996 Effect of bromide ion on haloacetic acid speciation resulting from chlorination and chloramination of aquatic humic substances. *Environ. Sci. Technol.* **30**, 16–24.

Duirk, S. E., Lindell, C., Cornelison, C. C., Kormos, J., Ternes, T. A., Attene-Ramos, M., Osiol, J., Wagner, E. D., Plewa, M. J. & Richardson, S. D. 2011 Formation of toxic iodinated disinfection by-products from compounds used in medical imaging. *Environ. Sci. Technol.* **45** (16), 6845–6854.

Gharekhanloo, F. & Torabian, S. 2012 Comparison of allergic adverse effects and contrast enhancement between iodixanol and iopromide. *Iran J. Radiol.* **9** (2), 63–66.

Giuseppe, M., Antonio, L., Huw, J. & Mike, F. 2007 By-products formation during degradation of isoproturon in aqueous solution. i: ozonation. *Water Res.* **7**, 1695–1704.

Gunten, U. 2003 Ozonation of drinking water: Part I. Oxidation kinetics and product formation. *Water Res.* **37** (7), 1443–1467.

Hennebel, T., De Corte, S., Vanhaecke, L., Vanherck, K., Forrez, I., De Gusseme, B., Verhagen, P., Verbeken, K., Van der Bruggen, B., Vankelecom, I., Boon, N. & Verstraete, W. 2010 Removal of diatrizoate with catalytically active membranes incorporating microbially produced palladium nanoparticles. *Water Res.* **44** (5), 1498–1506.

Hu, C. Y., Hou, Y. Z., Lin, Y. L., Li, A. P. & Deng, Y. G. 2019a Degradation kinetics of diatrizoate during UV photolysis and UV/chlorination. *Chem. Eng. J.* **360**, 1003–1010.

Hu, C. Y., Hou, Y. Z., Lin, Y. L., Deng, Y. G., Hua, S. J., Du, Y. F., Chen, C. W. & Wu, C. H. 2019b Kinetics and model development of iohexol degradation during UV/H_2O_2 and UV/$S_2O_8^{2-}$ oxidation. *Chemosphere* **229**, 602–610.

Hu, C. Y., Du, Y. F., Lin, Y. L., Hua, S. J., Hou, Y. Z., Deng, Y. G., Zhang, J. C., Ren, S. C., Dong, C. D., Chen, C. W. & Wu, C. H. 2020a Kinetics of iohexol degradation by ozonation and formation of DBPs during post-chlorination. *J. Water Process Eng.* **35**, 2214–7144.

Hu, C. Y., Hua, S. J., Lin, Y. L., Deng, Y. G., Hou, Y. Z., Du, Y. F., Dong, C. D., Chen, C. W. & Wu, C. H. 2020b Kinetics and formation of disinfection byproducts during iohexol chlor(am)ination. *Sep. Purif. Technol.* **243**, 1383–5866.

Huang, X. X., Quan, X. J., Cheng, W. & Li, J. 2020a Enhancement of ozone mass transfer by stainless steel wire mesh and its effect on hydroxyl radical generation. *Ozone Sci. Eng.* **42**, 347–356.

Downloaded from http://iwa.silverchair.com/jwrd/article-pdf/11/4/560/973551/jwrd0110560.pdf
by guest

Huang, Y., Luo, M., Li, S., Xia, D., Tang, Z., Hu, S., Ye, S., Sun, M., He, C. & Shu, D. 2020b Efficient catalytic activity and bromate minimization over lattice oxygen-rich MnOOH nanorods in catalytic ozonation of bromide-containing organic pollutants: lattice oxygen-directed redox cycle and bromate reduction. *J. Hazard. Mater.* **410**, 124545.

Ina, K., Hervé, G., Cynthia, J. & Jean-Philippe, C. 2009 The formation of halogen-specific TOX from chlorination and chloramination of natural organic matter isolates. *Water Res.* **43**, 4177–4186.

Jeong, C. H., Machek, E. J., Shakeri, M., Duirk, S. E., Ternes, T. A., Richardson, S. D., Wagner, E. D. & Plewa, M. J. 2017 The impact of iodinated X-ray contrast agents on formation and toxicity of disinfection by-products in drinking water. *J. Environ. Sci.* **58**, 173–182.

Jiang, J., Zhang, X., Zhu, X. & Li, Y. 2017 Removal of intermediate aromatic halogenated DBPs by activated carbon adsorption: a new approach to controlling halogenated DBPs in chlorinated drinking water. *Environ. Sci. Technol.* **51** (6), 3435–3444.

Jiang, J., Han, J. & Zhang, X. 2020 Nonhalogenated aromatic DBPs in drinking water chlorination: a gap between NOM and halogenated aromatic DBPs. *Environ. Sci. Technol.* **54** (3), 1646–1656.

Kormos, J. L., Schulz, M. & Ternes, T. A. 2011 Occurrence of iodinated X-ray contrast media and their biotransformation products in the urban water cycle. *Environ. Sci. Technol.* **45** (20), 8723–8732.

Li, X. F. & Mitch, W. A. 2018 Drinking water disinfection byproducts (DBPs) and human health effects: multidisciplinary challenges and opportunities. *Environ. Sci. Technol.* **52** (4), 1681–1689.

Liu, Z., Lin, Y. L., Xu, B., Hu, C. Y., Wang, A. Q., Gao, Z. C., Xia, S. J. & Gao, N. Y. 2018 Formation of iodinated trihalomethanes during breakpoint chlorination of iodide-containing water. *J. Hazard. Mater.* **353**, 505–513.

Mao, Y. X., Dong, H. Y., Liu, S. G., Zhang, L. P. & Qiang, Z. M. 2020 Accelerated oxidation of iopamidol by ozone/peroxymonosulfate (O_3/PMS) process: kinetics, mechanism and simultaneous reduction of iodinated disinfection by-product formation potential. *Water Res.* **173**, 115615.

Maryam, K., Ben, C., Cordwell, S. J., David, I. P. & Michael, J. D. 2020 Characterization of disulfide (cystine) oxidation by HOCl in a model peptide: evidence for oxygen addition, disulfide bond cleavage and adduct formation with thiols. *Free Radic. Biol. Med.* **154**, 62–74.

Meng, L., Yang, S., Sun, C., He, H., Xian, Q., Li, S., Wang, G., Zhang, L. & Jiang, D. 2017 A novel method for photo-oxidative degradation of diatrizoate in water via electromagnetic induction electrodeless lamp. *J. Hazard. Mater.* **337**, 34–46.

Michael, J. P., Mark, G. M., Susan, D. R., Francesca, F. & Occurrence, M. B. 2008 Synthesis, and mammalian cell cytotoxicity and genotoxicity of haloacetamides: an emerging class of nitrogenous drinking water disinfection byproducts. *Environ. Sci. Technol.* **42**, 955–961.

Nie, Y., Hu, C., Yang, L. & Hu, J. 2013 Inhibition mechanism of formation over MnO_x/Al_2O_3 during the catalytic ozonation of 2,4-dichlorophenoxyacetic acid in water. *Sep. Purif. Technol.* **117**, 41–45.

Perez, S. & Barcelo, D. 2007 Fate and occurrence of X-ray contrast media in the environment. *Anal. Bioanal. Chem.* **387** (4), 1235–1246.

Polo, A. M. S., López-Peñalver, J. J., Sánchez-Polo, M., Rivera-Utrilla, J., Velo-Gala, I. & Salazar-Rábago, J. J. 2016 Oxidation of diatrizoate in aqueous phase by advanced oxidation processes based on solar radiation. *J. Photochem. Photobiol. A: Chem.* **319–320**, 87–95.

Ranjan, J., Mandal, T. & Mandal, D. D. 2021 Mechanistic insight for DBP induced growth inhibition in *Vigna radiata* via oxidative stress and DNA damage. *Chemosphere* **263**, 128062.

Rathbun, R. E. 1996 Bromine incorporation factors for trihalomethane formation for the Mississippi, Missouri, and Ohio rivers. *Sci. Total Environ.* **192**, 111–118.

Richardson, S. D., Plewa, M. J., Wagner, E. D., Schoeny, R. & Demarini, D. M. 2007 Occurrence, genotoxicity, and carcinogenicity of regulated and emerging disinfection by-products in drinking water: a review and roadmap for research. *Mutat. Res.* **636**, 178–242.

Sandra Perez, P. E., Celiz, M. D. & Aga, D. S. 2006 Structural characterization of metabolites of the X-ray contrast agent iopromide in activated sludge using ion trap mass spectrometry. *Anal. Chem.* **78**, 1866–1874.

Shang, W., Dong, Z., Li, M., Song, X., Zhang, M., Jiang, C. & Feiyun, S. 2019 Degradation of diatrizoate in water by Fe(II)-activated persulfate oxidation. *Chem. Eng. J.* **361**, 1333–1344.

Song, R., Donohoe, C., Minear, R., Westerhoff, P., Ozekin, K. & Amy, G. 1996 Empirical modeling of bromate formation during ozonation of bromide-containing waters. *Water Res.* **30**, 1161–1168.

Sugihara, M. N., Moeller, D., Paul, T. & Strathmann, T. J. 2013 TiO_2-photocatalyzed transformation of the recalcitrant X-ray contrast agent diatrizoate. *Appl. Catalysis B: Environ.* **129**, 114–122.

Symons, J. M., Krasner, S. W., Simms, L. A. & Sclimenti, M. 1993 Measurement of THM and precursor concentrations revisited: the effect of bromide ion. *J. AWWA* **85**, 51–62.

Ternes, T. A., Stüber, J., Herrmann, N., McDowell, D., Ried, A., Kampmann, M. & Teiser, B. 2003 Ozonation: a tool for removal of pharmaceuticals, contrast media and musk fragrances from wastewater. *Water Res.* **37** (8), 1976–1982.

Velo-Gala, I., López-Peñalver, J. J., Sánchez-Polo, M. & Rivera-Utrilla, J. 2014 Comparative study of oxidative degradation of sodium diatrizoate in aqueous solution by H_2O_2/Fe^{2+}, H_2O_2/Fe^{3+}, Fe(VI) and UV, H_2O_2/UV, $K_2S_2O_8$/UV. *Chem. Eng. J.* **241**, 504–512.

Virmani, A., Walavalkar, M. P., Sharma, A., Sengupta, S., Saha, A. & Kumar, A. 2020 Kinetic studies of the gas phase reaction of 1,2-propylene oxide with the OH radical over a temperature range of 261–335 K. *Atmos. Environ.* **237**, 117709.

Von, G. U. 2003 Ozonation of drinking water: part II. Disinfection and by-product formation in presence of bromide, iodide or chlorine. *Water Res.* **37**, 1469–1487.

Wang, Z., Lin, Y.-L., Xu, B., Xia, S.-J., Zhang, T.-Y. & Gao, N.-Y. 2016 Degradation of iohexol by UV/chlorine process and formation of iodinated trihalomethanes during post-chlorination. *Chem. Eng. J.* **283**, 1090–1096.

Downloaded from http://iwa.silverchair.com/jwrd/article-pdf/11/4/560/973551/jwrd0110560.pdf
by guest

Xia, Y., Lin, Y. L., Xu, B., Hu, C. Y., Gao, Z. C., Chu, W. H. & Gao, N. Y. 2017 Iodinated trihalomethane formation during chloramination of iodate-containing waters in the presence of zero valent iron. *Water Res.* **124**, 219–226.

Yolanta, G., Tan, J., Allard, S., Heitz, A. & Bowman, M. 2014 Impact of bromide and iodide during drinking water disinfection and potential treatment processes for their removal or mitigation. *Water* **41**, 38–43.

Zhang, M., Wang, X., Hao, H., Wang, H., Duan, L. & Li, Y. 2019 Formation of disinfection byproducts as affected by biochar during water treatment. *Chemosphere* **233**, 190–197.

First received 15 June 2021; accepted in revised form 13 September 2021. Available online 30 September 2021

Downloaded from http://iwa.silverchair.com/jwrd/article-pdf/11/4/560/973551/jwrd0110560.pdf
by guest